Journal of Toyo University, Natural Science, No. 55 : 17 – 28 (2011)

Analysis of Soil Salinization and Alkalinization in the Songnen Plain of Northeast China

Katsutoshi SEKI*[1]

Abstract

Alkalinization and salinization of soil at Anda City, the Songnen Plain of Northeast China, were studied. The experimental plot was selected from salt-affected *Leymus chinensis* grassland, including an area of salt-accumulated soil having no grass on the surface. Soil physical and chemical properties were measured, and soil water content was monitored. The soil was very clayey, with both heavy clay and light clay. Saturated hydraulic conductivity was very low due to the clayey texture of the soil. The soil pH was higher than 8.5, and the EC of the soil water was more than 4 mS cm^{-1} at the surface, with a high Na^+ concentration; therefore, the soil was classified as saline-alkali. At the salt-accumulated, unvegetated area, pH and EC levels were higher than those at the vegetated area, indicating more severe soil alkalinization and salinization at the former area. The groundwater in this area has a high concentration of $NaHCO_3$, and the groundwater level rises about 50 cm during the rainy season. Due to the clayey soil and high groundwater table, the upward movement of salt and water from the salty groundwater to the soil surface is enhanced, leading to salinization and alkalinization. Continuous measurement of soil water content revealed that the soil water movement was different at the vegetated and unvegetated areas. At the unvegetated area, the soil water tended to become saturated at the longer period than the vegetated area where soil water was not always saturated because of plant water uptake.

Keywords: Salt accumulation, alkalinization, salinization, Songnen Plain

1. Introduction

The Songnen Plain of Northeast China, a 170,000 km^2 basin surrounded by mountains (Fig. 1), is now suffering from soil alkalinization and salinization, especially in the grasslands (Wang et al., 2009). The natural cause of the salinization is the wide distribution of alkali rock in the surrounding mountains (Lin et al., 2005). During the process of mineral weathering, bicarbonate forms and dissolves into the surface soil and ground runoffs of rainwater. As the soluble salts accumulate in groundwater, the salt concentration of the groundwater increases.

1) Faculty of Business Administration, Toyo University, 5-28-20 Hakusan, Bunkyo-ku, Tokyo 112-8606, Japan

Fig. 1 Map of Songnen Plain

The salt in the groundwater then accumulates in the soil surface by evaporation, causing the salinization problem. According to Lin et al. (2005), about 100 years ago, less than 5 % of grassland was salinized. However, Lie et al. (1998) report that about 20 % of the entire area of the Songnen Plain was salt-affected. The increase in the salt-affected land during the last 100 years indicates that the cause of the salinization is a result of not only natural causes but also human factors, i.e., increased population and grazing. The increase in grazing due to population pressure has led to the reduction of canopy cover throughout the grassland, the decrease of infiltration due to soil compaction and the decrease in evapotranspiration, causing saline groundwater to rise and surface soil salinity to increase (Wang and Ripley, 1997).

Richards (1954) classified salt-affected soil as saline soil, alkali soil and saline-alkali soil. Alkali soil and saline-alkaline soil, with a pH higher than 8.5, usually have a natric horizon which is rich in exchangeable sodium. Soils with a natric horizon are classified as Solonetz in the FAO soil classification.

The objective of this study is to analyze the mechanism of salt accumulation in the Songnen Plain. We focused on the mechanism of the formation of a patch-like salt crust area in this region. In the Songnen Plain, the patch-like distribution of the salt-crust area in the grassland is widely observed, suggesting that salinization is proceeding heterogeneously. In addition to analyzing why such a salt-crust distribution has formed and how water and salt move in these soils, we discuss the future fate of such salt soils.

Fig. 2 Salt accumulation.

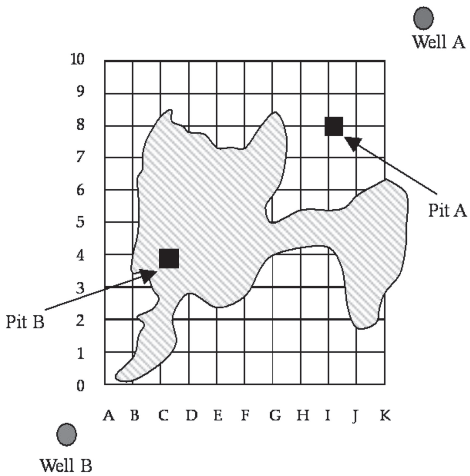

Fig. 3 Experimental plot with 3-m grid. Hatched part represents salt-accumulated bare soil.

2. Materials and Methods

2-1. Site description

The study site is an experimental grassland located at the Alkali Soil Natural Environmental Science Center of Northeast Forestry University, Anda City, Heilongjiang Province, China (Fig. 1).

The annual rainfall in this area is 350 mm, and more than 80 % of the rains occur mainly during the summer season between June and September. The annual potential evaporation estimated by the Thornthwaite model (Thornthwaite, 1948) is 540 mm. According to Xu et al. (2005), the annual potential evaporation estimated by Kondo and Xu's (1997) method is 788 mm at the nearby city of Harbin. Therefore, the annual potential evaporation is estimated to be higher than the annual rainfall in this region, suggesting that the upward movement of water in the soil is predominant.

While most of the study site was covered with grass, some patchy areas of bare soil with salt accumulated at the soil surface were observed (Fig. 2). An experimental plot of 30 m x 30 m was selected that covered both areas of bare soil with salt accumulation and areas covered with grass (Fig. 3). *Leymus chinensis* was the dominant grass species. At the edge of the salt-accumulated zone, salt-tolerant grasses were also found. The experimental plot was subdivided into a 3 m grid to depict the distribution of the salt-affected area accurately.

2-2. Soil properties

As shown in Fig. 3, two pits, each 1 m deep, were dug in the vegetated part (Pit A) and in the bare soil (Pit B) of the study site at the end of July 2006. The latter area had a salt crust of 3 mm thickness at the surface. Disturbed and undisturbed soil samples were taken and sent to a laboratory in Japan, where soil physical and chemical properties were measured. Soil texture was measured with disturbed samples by the wet sieve method and the bouyoucos hydrometer method and classified according to the system of the International Union of Soil Science. Water content was measured gravimetrically by oven drying the disturbed sample at 105 °C for 24 hours. Particle density was measured by a pycnometer method. With the undisturbed sample of a cylindrical core of 5 cm diameter and 5 cm height, saturated hydraulic conductivities were determined by the falling-head method, and the bulk densities were measured gravimetrically. From the values of water content, particle density and bulk density, the volumetric fractions of the solid, liquid and gas phases were calculated. With the disturbed samples, the pH was measured 30 minutes after the addition of distilled water to each soil sample in order to attain a 2:5 soil-water ratio. The soil and water were mixed well. Electrical conductivity (EC) was measured after the addition of distilled water to attain a 1:5 soil-water ratio. The surface soil was sampled at 3 m intervals (Fig. 3) from line C (third horizontal line from left) of the grid. Na^+, Ca^{2+} and Mg^{2+} concentrations were measured with the sample at a 1:5 soil-water ratio, and EC and pH were measured using the procedure described above.

2-3. Monitoring of groundwater level and volumetric water content

The annual change in the level of the groundwater table at two wells (Well A and Well B; Fig. 3) excavated at the experimental plot was monitored. Groundwater was sampled from the two wells, and the quality of the groundwater was analyzed. In the soil profile of Pits A

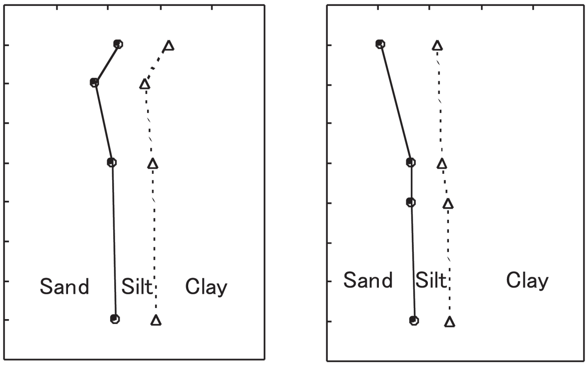

Fig. 4 Texture of soil at Pit A (left) and Pit B (right).

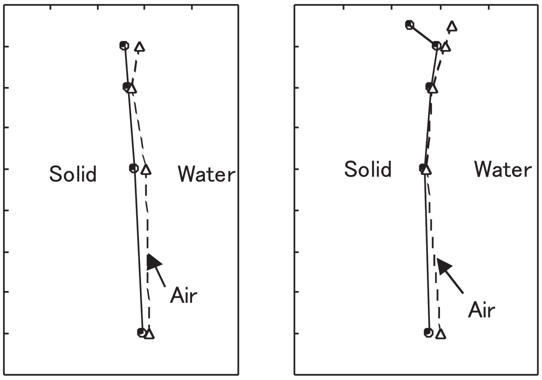

Fig. 5 Three-phase distribution of soil at Pit A (left) and Pit B (right).

and B, ECH_2O sensors (Decagon devices) for measuring water content were buried at specified depths: 5, 10, 20, 40 and 80 cm from the soil surface. The measured values were recorded automatically with data loggers at both pits. The sensors and the data loggers were buried in the soil from September 2005 to July 2006, and the annual change in the volumetric water content at each depth was recorded. The ECH_2O sensors were used to measure the dielectric permittivity of the soil in order to determine the volumetric water content of the soil. StowAway-TBI32 loggers (Onset) were also buried at depths of 10, 40 and 80 cm in the soil pits to measure temperature.

3. Results and Discussion

3-1. Soil physical properties

Many roots were observed in the top 15 cm layer, some roots were found at depths of 15 to 30 cm and a few roots were found below 30 cm. The soil texture is shown in Fig. 4. The soil was very clayey, with Pit B having much more clay than Pit A. At Pit A, the soil at a depth of

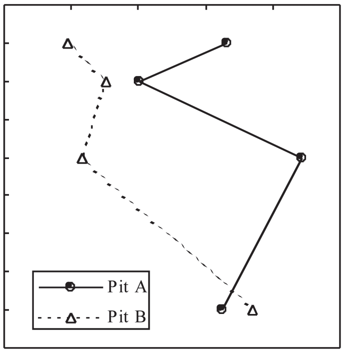

Fig. 6 Saturated hydraulic conductivity.

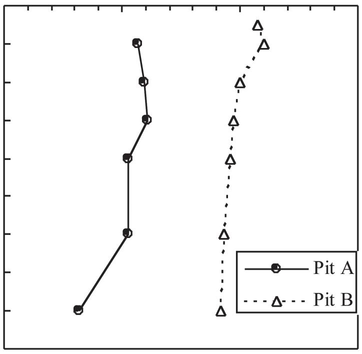

Fig. 7 pH (soil: water = 2:5).

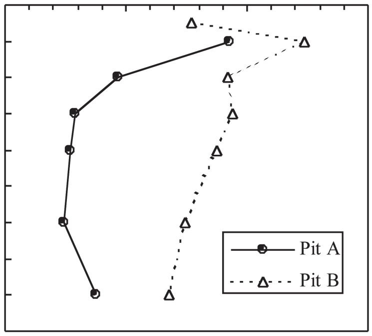

Fig. 8 EC (soil: water = 1:5).

20 cm was Heavy Clay, and the deeper soil was Light Clay. At Pit B, the soil profile was Heavy Clay. The three-phase distribution determined from bulk density, water content and particle density measurement is shown in Fig. 5. The soil was almost saturated throughout the soil profile, except at a depth of 5 cm at Pit B.

The saturated hydraulic conductivity is shown in Fig. 6. Hydraulic conductivity was low, reflecting the clayey texture of the soil. At the surface 40 cm layer of Pit B, hydraulic conductivity was especially low. Therefore, rainfall infiltration rate was low, and after a rainfall, water remained ponded for several days.

3-2. Soil alkalinization and salinization

Soil was alkalized throughout the soil profile at both pits (pH > 8.5); it was especially high (pH > 10) at Pit B, where there was bare soil at the surface (Fig. 7). EC was also high at the surface (Fig. 8). According to the classification of salt-affected soil by Richards (1954), soil having a pH higher than 8.5, as shown in Fig. 7, is classified as either alkali soil or saline-alkali soil. Richards' (1954) criterion for distinguishing between alkali and saline-alkali soils is the difference in EC. When the EC of the soil solution is lower than 4 mS cm^{-1}, the soil is classified as alkali, and when it is higher, it is classified as saline-alkali. Considering that the

Table 1 Groundwater quality.

	mmol/l	
	2005	2006
Na^+	5.65	5.09
K^+	0.0358	0.0332
Ca^{2+}	2.40	2.25
Mg^{2+}	1.56	1.40
Cl^-	0.846	0.874
HCO_3^-	7.57	7.51
F^-	0.0684	0.0779
$H_2SO_4^{2-}$	2.43	2.08
SiO_3^{2-}	0.201	0.208
pH	7.5	7.4
EC (mS/cm)	1.08	1.04

Table 2 Soil chemical properties at line C of the grid.

	mmol/l			EC (mS/cm)	pH
	Na^+	Ca^{2+}	Mg^{2+}		
C0	40.6	0.137	0.121	0.78	8.96
C1	83.8	ND	0.035	1.64	10.25
C2	52.5	ND	0.037	0.54	9.64
C3	74.1	0.0248	0.044	1.26	10.23
C4	89.0	ND	0.035	1.46	10.4
C5	135.8	0.103	0.161	1.95	10.3
C6	64.9	0.0317	0.053	0.94	10.34
C7	72.9	0.0279	0.047	1.05	10.21
C8	45.0	0.0070	0.040	0.72	10.14
C9	111.5	0.0334	0.077	1.63	10.35
C10	81.0	0.0075	0.086	1.18	9.53

EC in Fig. 8 was measured at a soil-water ratio of 1:5, the EC of the soil solution was estimated to be 5 times higher than the value shown in Fig. 8. The EC values of the surface soils at Pit A and Pit B both exceeded 0.8; i.e., the EC of the soil solution was higher than 4, and therefore the soil at Pit A and Pit B was classified as saline-alkali.

The area around Pit B, where there was a patch-like salt crust, had a clearly higher pH and electrolyte concentration than the adjacent vegetated area around Pit A (Figs. 7 and 8). Ma and Liang (2007) studied the growth of *Leymus chinensis* in soils having different pH values. When the pH was between 7.5 and 9.5, *Leymus chinensis* grew well even with salinized soil. When the pH was higher than 9.53, not much *Leymus chinensis* grew, and when the pH was higher than 9.86, all of the *Leymus chinensis* died within 50 days after planting. Therefore, a pH of 9.5 seems to be the crucial value, and when the pH exceeds 9.5, *Leymus chinensis* does not grow. At the vegetated area in this study, the pH was around 8.5 to 9, lower than the crucial value of 9.5. At the area of the salt crust, the pH was around 10, so grass could not survive. Therefore, it was confirmed that the patch-like formation of the salt crust was formed because of the difference in the current state of alkalinization. The heterogeneity of soil physical properties (more clayey soil at Pit B) may have been the cause of such heterogeneous alkalinization and salinization. The EC of the soil solution was 3 to 12 mS / cm (Fig. 8), much higher than the EC of the ground water of around 1 mS/cm (Table 1). The pH of the soil solution, 8.5 to 10, was higher than the pH of the ground water, 7.5.

The chemical properties of the surface soil, sampled at 3 m intervals (Fig. 3) from line C of the grid, denoted as C0, C1, ..., C10, are shown in Table 2. A high concentration of Na^+ accumulated at the surface, resulting in a high EC and pH.

3-3. Groundwater

The quality of the groundwater is shown in Table 1 as the average value of the groundwater taken from Wells A and B. The water had high concentrations of Na^+, Ca^{2+}, HCO^{3-} and $H_2SO_4^{2-}$. The changes in the groundwater level and rainfall data observed at the

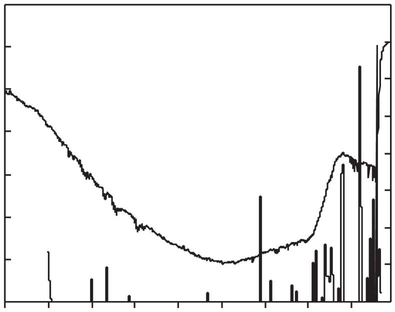

Fig. 9 Depth of groundwater table and precipitation.

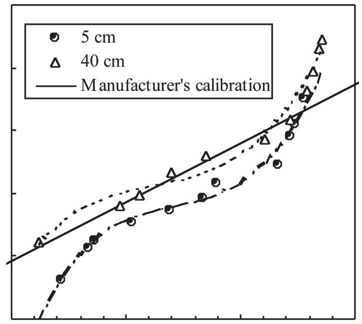

Fig. 10 Calibration curves of ECH2O sensors for soils in Pit B. Fitted curves are cubic functions.

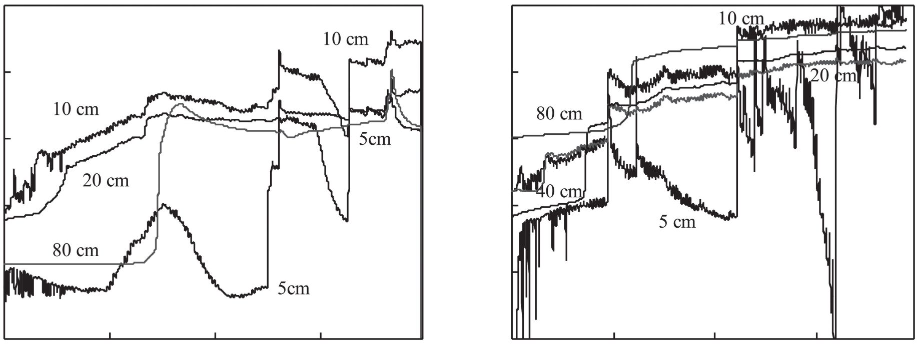

Fig. 11 Change in volumetric water content of Pit A (left) and Pit B (right).

adjacent city, Daqing, are shown in Fig. 9. The depth of the groundwater table was 2 m in January, and it gradually decreased to 3 m until April. After the snow melted at the beginning of April, the groundwater table rose gradually until the end of May. From the start of the rainy season, June, the groundwater rose with the rainfall, and at the end of July, the groundwater table reached a depth of 50 cm. As the groundwater table reached so close to the soil surface, the soil was almost saturated throughout the soil profile (Fig. 5). As the groundwater level increased during the summer, water moved upward by evaporation, and salt accumulated at the soil surface.

3-4. Change in soil water content

As the relationship between the dielectric permittivity and volumetric water content differs with soil type, calibration for the measurement of ECH_2O sensors was conducted in the laboratory with soil taken from the field. ECH_2O sensors are also affected by salt concentration; therefore, laboratory calibration was conducted with a $CaCO_3$ solution of 0.02 mol L^{-1} to minimize the discrepancy of the calibration curve from the field observation. Two of the calibration curves for the ECH_2O sensors are shown in Fig. 10. The general calibration

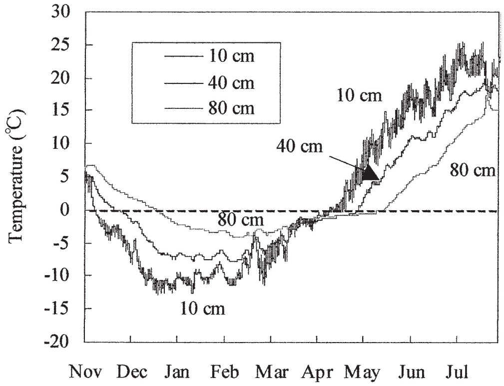

Fig. 12 Change in temperature of atmosphere and soil of Pit A.

given in the user's manual is also shown in the figure. The relationship between the sensor output and the volumetric water content was different from the manufacturer-distributed calibration curve, and they were also different for each soil sample. Therefore, the volumetric water content was calculated from the calibration curves of the cubic function obtained for each soil sample.

The change in soil water content is shown in Fig. 11. The ECH_2O sensors measured the dielectric permittivity to determine the volumetric water content. As the dielectric permittivity of frozen water is lower than that of unfrozen water, the apparent volumetric water content measured by ECH_2O sensors is lower than the true value when frozen water exists. The change in the soil temperature (Pit A) is shown in Fig. 12. In winter, the temperature of the soil is lower than the freezing point; therefore, the soil water is frozen. At the beginning of April, the ambient temperature rises above 0 °C, and the snow starts to melt. As predicted by the theory of heat flow with annual temperature fluctuation (Jury and Horton, 2004), the amplitude of the temperature change decreases with depth, and the pattern of the temperature change is delayed with depth. Therefore, the temperatures at soil depths of 10, 40 and 80 cm rose above the freezing point from the beginning of April to the middle of May. Lower volumetric water contents until this period in Fig. 11 could be attributed to the effect of soil freezing, and the values in this period do not represent the actual volumetric water content. Therefore, we mainly discuss the soil water change after the end of May.

At both Pit A and Pit B, the soil water content at a depth of 5 cm fluctuated greatly from May to the end of July, increasing with rainfall and decreasing with evaporation. At Pit A, the fluctuation of the soil water content was also observed at depths of 10 and 20 cm. At Pit B, soil water content continued to increase from May to July. After July, the water content at depths of 10 to 80 cm was kept high, and the water was almost saturated. At Pit A, as there was water uptake by the roots of the grass, the soil was not always saturated.

Acknowledgements

This study was funded by the Heiwa Nakajima Foundation. This study was conducted with Yoshio Ishihama, Shoichiroro Hamamoto, Dr. Takeshi Tokida, Dr. Li Wang, Hiromi Imoto, Dr. Masaru Mizoguchi and Dr. Tsuyoshi Miyazaki at the University of Tokyo. Dr. Shenkui Liu, Professor at the Alkali Soil Natural Environmental Science Center, Northeast Forestry University of China, helped us conduct field experiments.

References

Jury, W. A. and R. Horton. 2004. *Soil physics*, 6th edition. John Wiley & Sons, NJ, USA.

Kondo, J. and J. Xu. 1997. Seasonal variations in the heat and water balances for nonvegetated surfaces. *Journal of Applied Meteorology* 36: 1676-1695.

Li, Q. S., S. W. Qiu and W. Deng. 1998. Study on the secondary saline-alkalinization of land in the Songnen Plain. *Scientia Geographica Sinica* (in Chinese) 18(3): 268-272.

Lin, N. F., V. Bounlom, J. Tang and J. M. Bian. 2005. Study on the relation between the formation of saline-alkali soil and the Neotectonic Movement. *Global Geology* (in Chinese) 24(3): 282-288.

Ma, H. and Z. Liang. 2007. Effects of different soil pH and soil extracts on the germination and seedling growth of Leymus chinensis. *Zhiwuxue Tongbao* (in Chinise) 24(2): 181-188.

Richards, L. A. 1954. Diagnosis and improvement of saline and alikaline soils. Agriculture Handbook No. 60. United States Department of Agriculture, Government Printing Office, Washington D.C., USA.

Thornthwaite, C. W. 1948. An approach toward a rational classification of climate. *Geographical Review* 38: 55-94.

Wang, R. and E. A. Ripley. 1997. Effects of grazing on a Leymus chinensis grassland on the Songnen plain of north-eastern China, *Journal of Arid Environment* 36: 307-318.

Wang, L., K. Seki, T. Miyazaki and Y. Ishihama. 2009. The causes of soil alkalinization in the Songnen Plain of Northeast China. *Paddy and Water Environment* 7(3): 259-270.

Xu, J., S. Haginoya, K. Saito and K. Motoya. 2005. Surface heat balance and pan evaporation trends in Eastern Asia in the period 1971 - 2000. *Hydrological Processes* 19: 2161-2186.

要 旨

中国東北部松嫩平原における土壌のアルカリ化と塩類化の分析

関 勝寿 , Katsutoshi Seki

中国東北部松嫩平原の安達市における土壌のアルカリ化と塩類化の実態調査をした。試験地は塩類化した羊草（*Leymus chinensis*）の牧草地で、土壌表面への塩類集積によって裸地化した場所を含んでいる。土壌の物理化学性を測定し、土壌水分量の変動を連続測定した。土壌は粘土質で、土性区分は Heavy Clay と Light Clay であった。そのため、飽和透水係数は非常に低かった。土壌の pH は 8.5 よりも高く、EC は 4 mS cm^{-1} よりも高く、Na^{+} 濃度が高かったため、アルカリ塩性土壌であると判定された。塩類集積をして植生がなくなっている場所では、pH と EC が植生のある場所よりも高く、よりアルカリ化と塩類化が進行していることが示された。地下水には高濃度の $NaHCO_3$ が含まれ、雨期には地下水位が 50 cm にまで上昇する。土壌が粘質で地下水位が高いため、地下水が地下水中に含まれる塩分とともに地表まで毛管上昇し、土壌の塩類化とアルカリ化を引き起こす。土壌水分量の連続測定により、植生のある場所とない場所では土壌水分移動の様子が異なることが分かった。植生のない場所では、植生のある場所と比べて土壌が飽和している期間が長く、それは植生のない場所では植物が水を吸水しているためと考えられた。